Persistent breathers in long-ranged discrete nonlinear Schrödinger models

C. Brunhuber* and F. G. Mertens
Physikalisches Institut, Universität Bayreuth, D-95440 Bayreuth, Germany

Y. Gaididei
Bogolyubov Institute for Theoretical Physics, 03143 Kiev, Ukraine
(Received 16 February 2006; published 18 May 2006)

The DNLS model including Kac-Baker long-range interactions and nonlinear damping exhibits prominent effects in computer simulations. The combination of long-range forces and damping yields a periodic pattern of stationary breathers from an originally uniformly distributed background. The inverse interaction radius determines the periodicity which can be understood in the quasicontinuum approximation of the system. For the undamped system, we investigate the impact of the long-range interactions on the transition to the persistent-breather phase, which only depends on the energy and the norm of the DNLS. Using Monte Carlo techniques, we can monitor the localization strength as a function of the the long-range radius and the system temperature, which is formally negative in the persistent-breather phase.

DOI: 10.1103/PhysRevE.73.056610 PACS number(s): 05.45.Yv, 05.10.Ln

I. INTRODUCTION

Discrete nonlinear systems have become a topic of intensive theoretical and experimental research [1]. They appear in various fields of traditional physical research (energy localization in solids, behavior of amorphous materials [2], Bose-Einstein condensates [3]) as well as in relatively new subdisciplines like biophysics (denaturation of DNA [4], biopolymers [5], self-trapping of vibrational energy in proteins [6]) or more technical applications (optical waveguide arrays [7], Josephson junctions [8]). The last two decades were above all labeled by the aim to understand the properties of the intrinsic localized modes (or discrete breathers), very robust solutions of nonlinear lattice equations, which were shown to exist for any sufficiently discrete nonlinear lattice. Recent reviews treat the discrete nonlinear Schrödinger equation (DNLS) and sum up the most important results about breather stability, their mobility, and their interactions (with themselves and with phonons) [9,10]. Realistic models usually lead to more complicated equations than the unperturbed lattice equation. Examples are noise terms and damping terms which arise to represent the effects of a thermal bath, e.g., in the theory of molecular monolayers for $T>0$ [11,12]. Curvature effects [13] and more complicated interaction potentials than nearest neighbor coupling are sometimes inherent when one wants to describe realistic models, e.g., with dipole-dipole or Coulomb forces [14,15]. Up to now, the perturbations were usually regarded from the perspective of its effect on the breather solution [12,16] but there was also some work done on the statistical mechanics of DNLS systems where the main focus is to explain the formation of persistent breathers. It was found that the DNLS system shows a phase transition from the Gibbsian regime to the regime of persistent breathers which formally corresponds to negative temperatures [17,18]. A different approach showed that this phenomenon is typical for systems with two conserved quantities and that the formation of persistent breathers maximizes the entropy of the system [19–21].

A long-range DNLS model corresponds formally to a discrete self-trapping equation (DST) which was proposed in 1985 by Eilbeck *et al.* to describe the self-localization process of CO vibration energy in natural proteins [22]. The DNLS equation resembles the limit of the DST when only nearest neighbor coupling is assumed, whereas the DST allows a dispersive coupling between all the oscillators stemming from their electromagnetic interactions [23]. The relevance of nonlinear excitations in biomolecules has been an object of strong controversy in the last decades [6]. Recently, a direct observation of self-trapped states in pump-probe experiments of a model protein (ACN) showed that the self-trapping could describe some important features of proteins (although the lifetime of the excitation in isolated molecules is shorter than expected by Davydov) [24].

In this paper, our main interest is to investigate the influence of long-range forces and damping on the formation of breather structures in the DNLS. The long-range forces are of the Kac-Baker-type, a harmonic coupling between the oscillators which depends exponentially on their distance. The parameter α, the inverse radius of the long-range interaction, represents a tunable parameter which mediates between the limits of nearest neighbor coupling ($\alpha\to\infty$) and the limit in which each lattice point is directly connected to every other point on the lattice ($\alpha\to 0$). The influence of the long-range forces in the DNLS yields some interesting effects concerning the stability of the solutions (see [15] and references therein). For the dissipation, we introduce nonlinear damping which has the property to conserve the excitation number of the DNLS. The nonlinear damping was derived from the Davydov model for energy transport in a nonlinear model for monolayer Scheibe aggregates [11,12]. We aim to describe the effect of long-range interactions and nonlinear damping on the DNLS lattice. In our studies, we numerically verify

*Electronic address: Christian.Brunhuber@uni-bayreuth.de

the strong effect of damping and long-range forces by measuring quantities like the localization strength of the norm or the mean distance between breathers. Long-range interactions are fundamental in the study of many physical systems like in astrophysics, nuclear physics, metallic clusters, and Bose-Einstein condensates and lead to phenomena like phase transitions or thermodynamical anomalies [25]. Therefore, we also revisit the undamped system in order to clarify the role of the long-range forces on the thermodynamics of the system and the transition into the regime of persistent breathers formation. Although we could not give a complete analytical description of the DNLS system with long-range forces and damping, we succeed in explaining the qualitative behavior of the system.

II. THE MODEL

The model is a DNLS equation where the dispersive interaction is nonlocal and nonlinear damping is included

$$2i\omega_o\dot{\phi}_n - \sum_m J_{n-m}(\phi_n - \phi_m) + 3B|\phi_n|^2\phi_n - \gamma\phi_n(|\phi_n|)_t = 0. \tag{1}$$

The DNLS has one conserved quantity $\mathcal{N}$, the norm

$$\mathcal{N} = \sum_n |\phi_n(t)|^2, \tag{2}$$

and the Hamiltonian

$$H = \sum_{n=1} -\frac{3}{4}\frac{B}{\omega_o}|\phi_n|^4 + \frac{1}{2}\sum_{m=1}\frac{J_m}{\omega_o}|\phi_n - \phi_{m+n}|^2 \tag{3}$$

which is only conserved for $\gamma=0$ and describes a Klein-Gordon-type lattice of oscillators with an attractive nonlinear term,

$$H_{\mathrm{KG}} = \sum_n \frac{\dot{u}_n^2}{2} + \frac{1}{2}\sum_{n,m} J_{n-m}(u_n - u_m)^2 + \sum_n \frac{\omega_o^2}{2}u_n^2 - \sum_n \frac{B}{4}u_n^4 \tag{4}$$

in the rotating wave approximation for $u_n(t)=\phi_n(t)\times\exp(-i\omega_o t)+\mathrm{c.c.}$ [26]. We choose the nonlocal interaction of the Kac-Baker-type,

$$J_m = J(\alpha,N)e^{-\alpha|m|} = J\frac{(e^\alpha - 1)}{(1 - e^{-\alpha N})}e^{-\alpha|m|}, \tag{5}$$

$$\sum_m^N J_m = J, \tag{6}$$

which makes it possible to cover the scenario of nearest neighbor ($\alpha\to\infty$) and all-to-all coupling ($\alpha\to 0$). The inclusion of a nonlinear damping term $\gamma\phi_n d/dt|\phi_n|^2$ in (1) enables a dissipative mechanism but keeps the norm (or the number of particles) constant. This damping term arises naturally when one reduces the Davydov equations for an exciton in a phonon bath to a DST-type equation for only the excitation amplitude [27] and is mathematically similar to Raman losses in the field of nonlinear optics. Solutions for this equation were also found in the quasicontinuum approximation (QCA) of the undamped DNLS and it was stated among other things that one can observe the collapse of the wave function for some initial conditions [28].

We want to stress the fact that a smaller α does not simply introduce a stronger effective coupling than for larger α. The condition (6) ensures a smaller coupling when the interaction radius grows and the effects we see in the simulations are purely due to the new length scale α^{-1}.

III. SIMULATIONS

We initialize the system with a uniformly distributed norm and a small perturbation. We choose either the case of just one deviating particle or a small random perturbation for all particles,

$$\text{case I: } \phi_{n\neq n_1}(0) = \sqrt{a}, \quad \phi_{n_1} = (1+\epsilon)\sqrt{a}, \tag{7}$$

$$\text{case II: } \phi_n = \sqrt{a} + \epsilon ranf(). \tag{8}$$

In the simulations, we always choose ($\omega_o^2=A=1$) and for the damping quite arbitrarily $\gamma=1$. Smaller values just seem to lengthen the transition to the stationary profile of the system.

In Fig. 1, we can clearly see several important consequences of the increase of the long-range forces. First, the length scale of the breather pattern grows with the interaction radius α^{-1}, the breathers become very intensive for small α, and the spatial expansion of the regular pattern (starting at $n_1=300$) is faster for small α. The effect of the damping becomes clear when we (qualitatively) compare our simulations with studies of undamped DNLS systems, e.g., in [20] where the breathers have a strong tendency to mix in order to create an entropically favorable state of persistent high-amplitude breathers.

The initial condition II leads to a very similar pattern with regards to the breather intensities and their number in the system (see Fig. 4 below). A rather remarkable fact which cannot be seen in the two pictures is the different behavior at the time when the breathers begin to form. Although the time for the breather formation does not depend on α, the formation of the breathers resembles more and more a quasicollapse process for small values of α where the energy of the system suddenly locates at the breather centers, a fact that is supported by the observations in [28] for the same system in the quasicontinuum approximation (without damping).

If we choose larger values of J, we increase the coupling and the transfer of the norm is even more efficient and the above described effect gets more drastic. In the case of $\alpha=0.2$ and $J=1=10B$, we are already in the situation where the whole norm of the system streams to two "hot spots." We can take the $J=1$ situation as an example to take a closer look at the collapsing in the DNLS. In Fig. 2, we obtain for $J=1$ at first two broad excitations. During the collapse, all the norm of each excitation gathers at its central site. For an $\alpha=0.2$ [Fig. 2(a)] we end up with a final state where all the norm of the system gathers at two very high-amplitude hot-spots [note the scale in Fig. 2(a)] The collapse can be

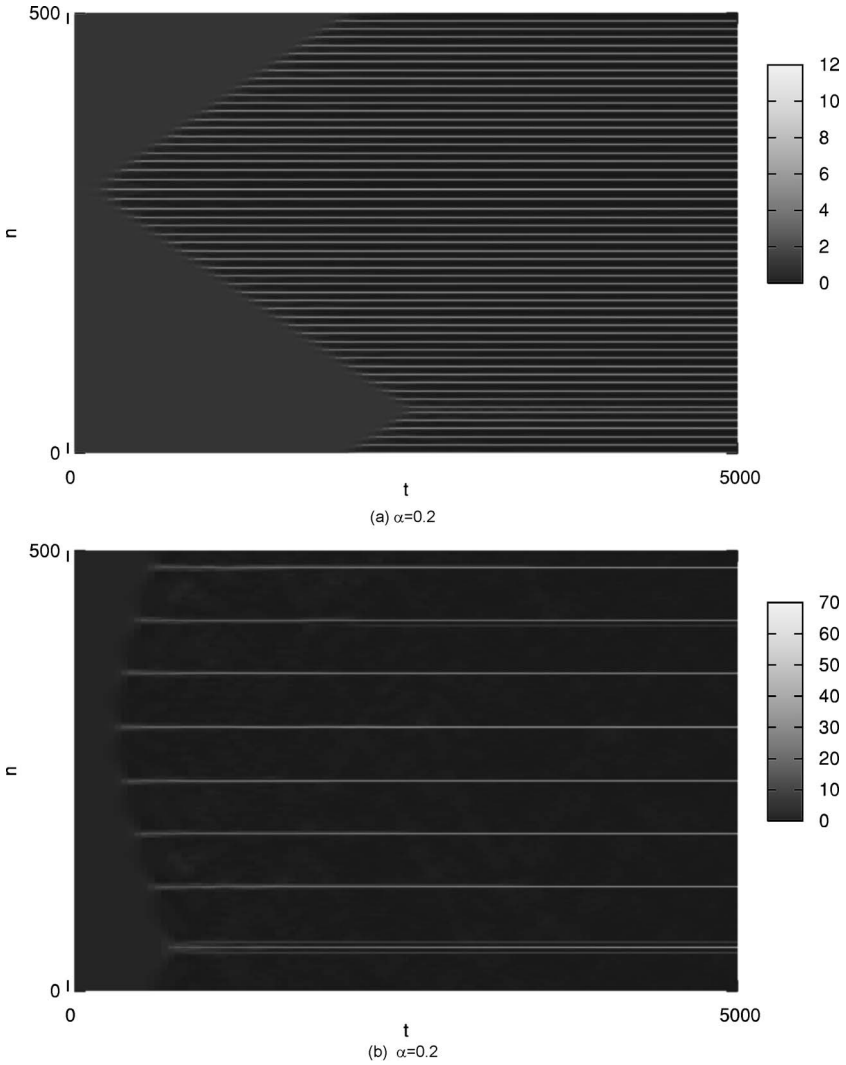

FIG. 1. Evolution of $|\phi_n(t)|^2$ for the DNLS equation ($B=0.1$, $J=0.1$, $\gamma=1$) with $\alpha=2$ (a) and $\alpha=0.2$ (b) for initial condition I. The pattern displays the norm of each lattice site $|\phi_n(t)|^2$ for 5000 time steps in units of the average norm $a=0.16$.

avoided when we reduce the norm of the system, e.g., the same simulation with $N=500$ instead of $N=512$ ($\mathcal{N}$ is reduced by $12a$) runs into an end state where the two broad excitations do not collapse. We have a situation where the breathers are very broad. Here the results from the quasicontinuum approximation in [28] should be applicable.

The system in Fig. 1 looks quite stationary after 5000 time steps but there are still smaller excitations and breathers in the dark area between the large breathers. For long times, the pattern gets clearer, the smaller breathers disappear for the benefit of the larger ones and maybe sometimes breathers grow for a while but later, when there are no more smaller breathers, they begin to shrink themselves. For small α it takes quite long to reach a stationary profile. Running simulations for many different values of α and for long times ($\sim 10^5$ time steps) we can measure the mean distance between the remaining breathers, which grows linearly with α^{-1} (Fig. 3). This confirms our expectation that the mechanism of the pattern formation consists of creating one hot spot for characteristic regions on the lattice which scale like α^{-1}. The main goal of the next section is to develop a qualitative understanding of the results displayed in Fig. 3, namely, the linear dependence of the average breather distance l on J and α^{-1}.

IV. QUASICONTINUUM APPROXIMATION

The full dynamics of the system (1) is quite complicated because discreteness, long-range effects, and damping are important for the dynamics. Nevertheless, we will win some insight into the breather formation when we consider the system in the quasicontinuum approximation. Our main goal is to explain the linear dependence of the mean breather distance on the parameters J and α^{-1} when the system has reached a stationary state. Here we will use one of the main results of [28], namely that the norm of a solution of a nonlocal NLS for one fixed value of α is related to the norm for a different α by a simple scaling relation. The QCA is an appropriate tool because in the process of the norm localization (starting from a uniformly distributed norm of the system), the system first develops very broad bell-shaped structures which then become more and more narrow [Fig. 2(b)]. Naturally the final stage of this process cannot be described by a continuum approximation, but we do not need this stage for the following considerations. We can also neglect the role of the nonlinear damping when we consider the stationary state of the system. The role of the nonlinear damping is, qualitatively speaking, the purification of a stationary profile because rapid temporal fluctuations of the quantity $|\phi_n(t)|$

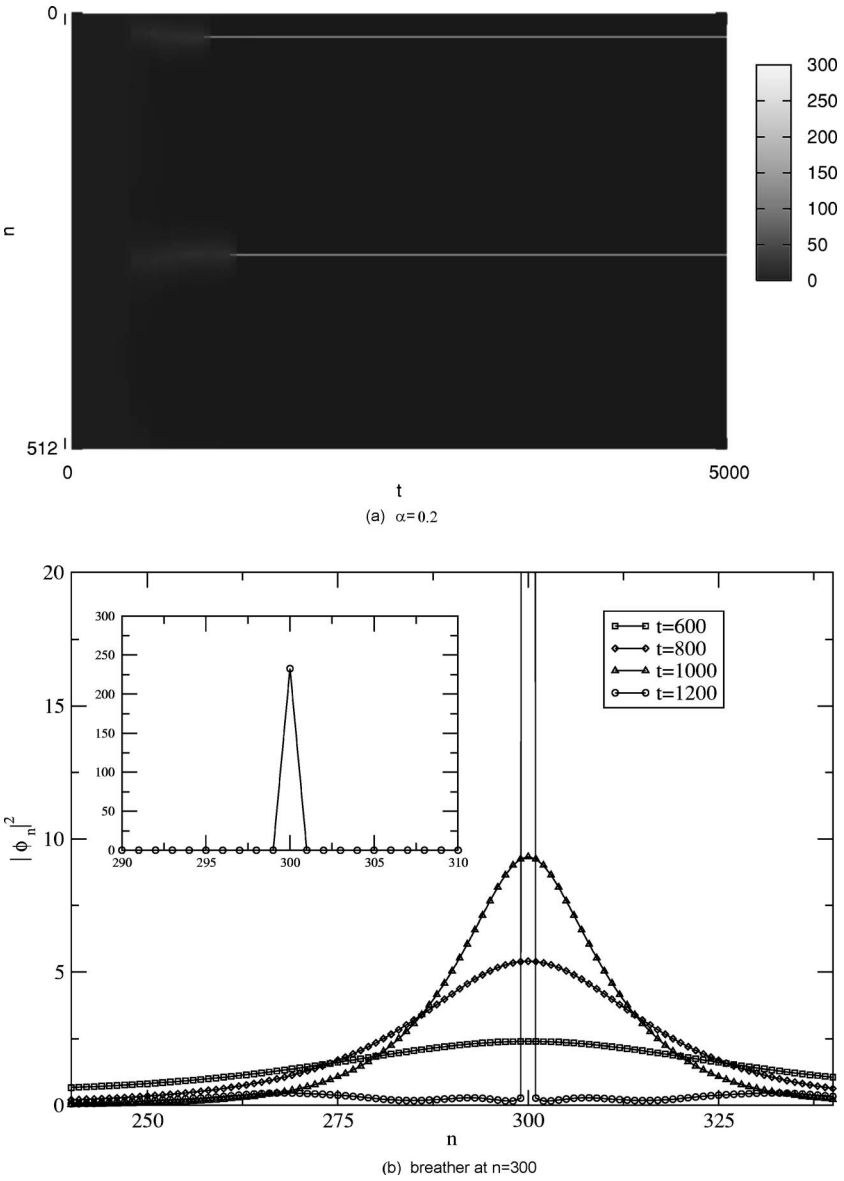

FIG. 2. Evolution of $|\phi_n(t)|^2$ for the DNLS equation ($B=0.1$, $J=1$, $\gamma=1$) with $\alpha=0.2$ and initial condition I (a). After some time, very broad excitations form at $n=300$ and $n=50$ and show a quasicollapse where almost all the norm of the breathers gathers in the central sites (b).

will be damped away. In this way the system gets rid of linear excitations and favors the creation of stationary solutions which are characteristic for DNLS equations. The effect of the nonlinear damping disappears for the stationary profile and the observed breather solutions are determined only by the parameters J, α, and B.

In order to estimate the norm of one of these stationary breathers, we go to the QCA $[n\to x,\ \phi_n(t)\to\phi(x,t)]$ where the system (1) can be described by a nonlocal nonlinear Schrödinger equation (NLS) of the form

$$i\partial_t\phi+\frac{2J(\alpha,N)}{\alpha}\frac{\partial_x^2}{\alpha^2-\partial_x^2}\phi+|\phi|^2\phi=0, \tag{9}$$

with the scaling $\phi\to\sqrt{2/3B}\phi$, $J\to J/2$ and neglecting the nonlinear damping term. Scaling space, time and the field ϕ $[z=\alpha x,\ \tau=2J(\alpha,N)/\alpha t,\ \psi=\sqrt{\alpha/2J}\phi]$ leads to

$$i\partial_\tau\psi+\frac{\partial_z^2}{1-\partial_z^2}\psi+|\psi|^2\psi=0. \tag{10}$$

This equation was solved by Gaididei *et al.* [28] by the ansatz

$$\psi=\frac{b}{\sqrt{b^2-1}}F(z,b)e^{i\lambda^2\tau}, \tag{11}$$

where λ is the spectral parameter of the soliton and $b=\lambda^{-1}\sqrt{\lambda^2+1}$ the width of the soliton. $F(z,b)$ could only be given in implicit form for $b\geqslant 3$, but the norm could be calculated as

$$\mathcal{N}_\phi=\int_{-\infty}^{\infty}|\phi(x,t)|^2dx=\frac{2}{3B}\frac{J(\alpha,N)}{\alpha^2}\mathcal{N}_\psi, \tag{12}$$

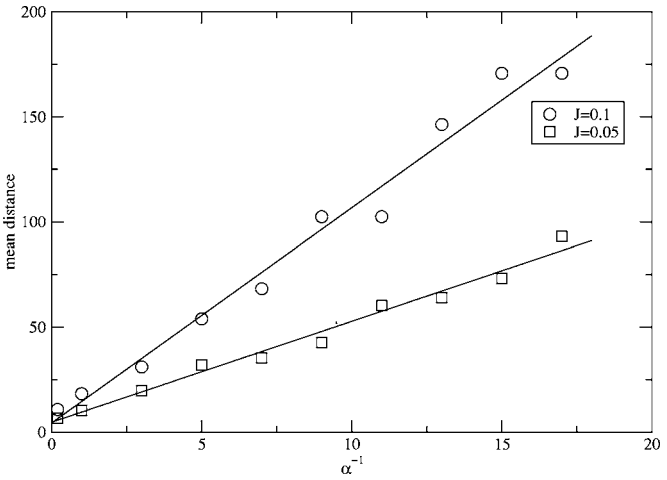

FIG. 3. Average distance between the breathers in the end state of the system ($N=1024$, $\gamma=1$, $B=0.1$ and $J=0.1$ or $J=0.05$) for different values of α. The mean breather distance scales linearly in α^{-1} and the slope of the curves increases with J. The full line fits the data points with a slope 4.803 ± 0.225 for $J=0.05$ and 10.233 ± 0.516 for $J=0.1$. For $\alpha^{-1}=17$, the time to reach a state where all the small breathers have vanished is about 10^5 time units.

$$\mathcal{N}_\psi = \int_{-\infty}^{\infty} |\psi(z,\tau)|^2 dz = \frac{1}{b^2-1}\left[3b + \frac{b^2-9}{8}\ln\left(\frac{b^2+4b+3}{b^2-4b+3}\right)\right]. \quad (13)$$

Assuming that the norm $\mathcal{N}$ of the system is shared by Z identical solutions (the same b, the same $\mathcal{N}_\psi$)

$$\mathcal{N} = Z\mathcal{N}_\phi = Z\frac{2}{3B}\frac{J(\alpha,N)}{\alpha^2}\mathcal{N}_\psi, \quad (14)$$

the mean breather distance l can now be estimated for small values of α as the total system length $L=N$ divided by the breather number Z

$$l = \frac{N}{Z} = \underbrace{\mathcal{N}_\psi \frac{2}{3a(1-e^{-\alpha N})}}_{\text{const. for } N\gg\alpha^{-1}} J\frac{e^\alpha - 1}{B\alpha^2} \sim \frac{J}{B}\alpha^{-1}. \quad (15)$$

This explains the results of Fig. 3, the linear dependence of the mean breather distance on the parameters J and α^{-1}! The results for l from the simulations are in good qualitative agreement although we did not consider the damping and assumed that we would end up in a sequence of Z regions with the same norm $\mathcal{N}_\phi$ which is in general not true. There are always breathers with higher and lower intensity. Another problem in obtaining the data points in Fig. 3 is that we were not able to run the simulations on very long chains ($N\gg l$) which is necessary in the case of small α in order to get good statistics for the mean breather distance (simulation time $\sim N^2$ for long-range systems).

We can estimate the critical norm $\mathcal{N}_\phi^c$ of the DNLS with the result from [28] for the critical norm of the NLS soliton ($\mathcal{N}_\psi^c \simeq 1.128$) using the formula (14). This means for the parameter values of the simulation in Fig. 2, the collapse of $Z=2$ excitations should occur for a norm $\mathcal{N}\geqslant 2\mathcal{N}_\phi^c = 83.25$. The collapse occurs in the simulation already for the norm $\mathcal{N}=Na=512\times0.16=81.92$ but not for the smaller system with $\mathcal{N}=Na=500\times0.16=80$. So, the QCA gives us a good estimate for the critical norm of the system.

We should keep in mind that the long-range interaction (small α) generally favors the collapse in the DNLS and a large ratio J/B leads to massive excitations (but on the cost of their number Z).

V. THE DIMER

Our model allows us to consider the limits of nearest neighbor coupling ($\alpha\to\infty$) and equal coupling between all sites ($\alpha\to0$). We want to use the latter case in order to get some insight into the dynamics of our system for large interaction radius α^{-1} and the norm-localization mechanism from a uniform background. The system of N particles behaves (for the initial condition I) like a dimer with the sites ϕ_{n_1} and $\phi_{n\neq n_1}$,

$$J_m = J\frac{(e^\alpha-1)}{(1-e^{-\alpha N})}e^{-\alpha m} \overset{\alpha\to0}{\approx} \frac{J}{N}. \quad (16)$$

The Hamiltonian (omitting a constant term and without damping) can be written as

$$H^D = -\frac{1}{4\omega_o}\frac{J}{N}\sum_{n,m\neq n}^{N}(\phi_m\tilde{\phi}_n + \phi_n\tilde{\phi}_m) - \frac{3B}{4\omega_o}\sum_{n}^{N}|\phi_n|^4. \quad (17)$$

The corresponding equation of motion with an additional term for the nonlinear damping [like in (1)] reads

$$2i\omega_o\dot{\phi}_n + \frac{J}{N}\sum_{m\neq n}^{N}\phi_m + 3B|\phi_n|^2\phi_n - \gamma(|\phi_n|^2)_t\phi_n = 0. \quad (18)$$

Since only the site n_1 deviates (infinitesimally) from the value $\phi_{n\neq n_1}=\sqrt{a}$, the system of N particles can be written as a dimer equation set where ϕ_o is the deviating site at n_1 and all the other sites are described by ϕ_1. After the transformations $\phi_o := \phi_{n_1} = \sqrt{N-1}\,\bar{\phi}_o$, $\phi_1 := \phi_{n\neq n_1} = \bar{\phi}_1$, the dimer equation set reads

$$i\dot{\bar{\phi}}_o = -\bar{J}\bar{\phi}_1 - \bar{V}_o\bar{\phi}_o\bar{\rho}|\bar{\phi}_o|^2, \quad (19)$$

$$i\dot{\bar{\phi}}_1 = -\bar{J}\bar{\phi}_o - E_1\bar{\phi}_1 - \bar{V}_1\bar{\phi}_1\bar{\rho}|\bar{\phi}_1|^2, \quad (20)$$

with

$$\bar{J} = \frac{J\sqrt{N-1}}{2N}, \quad \bar{V}_o = \frac{3}{2}B(N-1),$$

$$\bar{\rho} = \left(1 - \frac{\gamma}{3B}\frac{d}{dt}\right), \quad E_1 = \frac{J(N-2)}{2N}, \quad \bar{V}_1 = \frac{3}{2}B. \quad (21)$$

If we substitute [27]

$$\bar{\phi}_o^{\,*}\bar{\phi}_1 + \bar{\phi}_o\bar{\phi}_1^{\,*} = \sin\Theta\cos\Psi = x(t), \tag{22}$$

$$-i(\bar{\phi}_o^{\,*}\bar{\phi}_1 - \bar{\phi}_o\bar{\phi}_1^{\,*}) = \sin\Theta\cos\Psi = y(t), \tag{23}$$

$$|\bar{\phi}_o|^2 - |\bar{\phi}_1|^2 = \cos\Theta = z(t), \tag{24}$$

$$\bar{\mathcal{N}} = |\bar{\phi}_o|^2 + |\bar{\phi}_1|^2 = \frac{\mathcal{N}}{N-1}, \tag{25}$$

we end up with the equations,

$$\dot{\Psi} = \frac{2\bar{J}z\cos\Psi}{\sqrt{\bar{\mathcal{N}} - z^2}} - \frac{\bar{V}_o - \bar{V}_1}{2}\bar{\mathcal{N}} - \frac{\bar{V}_o + \bar{V}_1}{2}\bar{\rho}z, \tag{26}$$

$$\dot{z} = -2\bar{J}\sqrt{\bar{\mathcal{N}} - z^2}\sin\Psi. \tag{27}$$

This set is analytically solvable for $\gamma=0$ and yields low-amplitude oscillations of $z(t)$ around the start value. If one includes damping, one can numerically solve the system and we get a growing $z(t)$ from its start value $z(0)\approx-\bar{\mathcal{N}}$ when the norm $|\phi_o|^2$ differs slightly from $|\phi_1|^2$ to its maximum value $z(\infty)=\bar{\mathcal{N}}$ when all the norm is at one site ($|\phi_o|^2=\mathcal{N}$). This result has the following interpretation:

For the case of a dimer ($\alpha\to 0$ and initial conditions I), the system has the tendency to transfer norm to the site ϕ_{n_1} from all the other sites. For finite α, the system develops ripples in its early state which grow at the expense of the surrounding sites (α^{-1} scale), qualitatively something like a sequence of "almost dimers." The collapse dynamics of the system takes place on a length scale of one lattice constant and can of course not be modeled within the dimer approximation.

VI. THERMALIZATION

Most studies of the role of breathers in DNLS systems regard the interaction of breathers with the noisy small-amplitude background of the system [16,29]. It is known that DNLS breathers can be spontaneously created from a noisy background similarly as it was reported for Klein-Gordon lattices [30], modeling DNA-chains, or Fermi-Pasta-Ulam (FPU) lattices [31]. First, a creation of a large number of small amplitude breathers from the initial conditions occurs (like the modulational instability of traveling plane waves). The second step in the energy localization process is much more time consuming and consists of inelastic collisions between breathers where the larger breathers show the tendency to grow at the expense of the smaller ones. For FPU systems, long-time simulations revealed that there is an additional feature, namely the destruction of breathers by the phonon oscillations which lead to the equipartition of energy [31]. A quantitate understanding which kinds of spatially extended initial conditions lead to the formation of persistent localized modes requires a statistical-mechanics description [17]. As a result of this study, one can keep in mind that the mechanism is basically that of an "overheated" system with (microcanonical) $T<0$ which cools itself by creating "hot spots" of localized energy. In the microcanonical ensemble (fixed $\mathcal{N}$, H, and N) it was shown that the process is entropically driven in the sense, that the system at $\beta=0$ (β is the inverse temperature) presents a maximum entropy state and further energy input is shifted to some "hot spots" in order to preserve the favorable small-amplitude state for the other sites.

Here, we try to investigate the influence of the long-range forces on the statistics of the undamped DNLS system ($\gamma=0$) and therefore we define the quantity

$$\eta = N\frac{\sum_i^N |\phi_i|^4}{(\sum_i^N |\phi_i|^2)^2} \tag{28}$$

as an indicator of the localization of the norm in the system. The value of η lies in the interval $[1,N]$ between the situation of uniformly distributed norm and the situation where all the norm of the system is at one site. This quantity is not able to tell us at which site the persistent breathers appear in the system, so we also computed in our simulations the probabilities p_n of finding the norm unit $a=\mathcal{N}/N$ at one site. The inclusion of the dispersive long-range potential results in a few important changes for the above explained thermalization scenario (we use the initial conditions II). The long enduring period of breather collisions for $\alpha=5$ [Fig. 4(a)] is for smaller values of α replaced by a faster process where high-amplitude breathers grow by extracting energy from their neighborhood (defined by the α^{-1}-scale) [Fig. 4(b)]. Sometimes a smaller breather which runs parallel to a larger one gets absorbed without changing positions [Fig. 4(b)]. Moreover, the localization parameter η after long times is distinctly larger for smaller values of α. Another feature is again the collapse process. For small values of α the pattern (the $|\phi_n|^2$ distribution) at the collapse time is much clearer, the breathers are arranged quite regularly. For later times this regular structure (which was conserved in the case of nonzero damping) merges into a more marbled pattern.

In [17,18] the probability $p(A_n)$ of a particle in the DNLS equation to possess a certain norm $|\phi_n|^2=A_n$ ($\phi_n(t)=A_n(t)\exp[i\theta_n(t)]$) was calculated by using the transfer integral method (assuming an infinite system). The evaluation of $p(A_n)$ for $\beta\to 0$ yielded some interesting conclusions which makes the quantity $p(A_n)$ a reliable indicator for the transition to negative temperatures. It was stated that in the case $\beta=0$, the logarithm of $p(A_n)$ is linear in A_n [$\log p(A_n)\sim-\Gamma A_n$] where $\Gamma=\beta\mu$ and the curvature of $p(A_n)$ becomes negative (positive) for positive (negative) temperatures. Here μ is the chemical potential which results from the interpretation of $\mathcal{N}$ as a particle number. This behavior was confirmed by long-time simulations of the DNLS [18] by averaging the values A_n over many time instances. In the case of negative temperatures, it was shown that $p(A_n)$ has a linear slope for small A_n, a feature which confirms the ansatz of Rumpf [20] to separate the phase space in a low- and high-amplitude part.

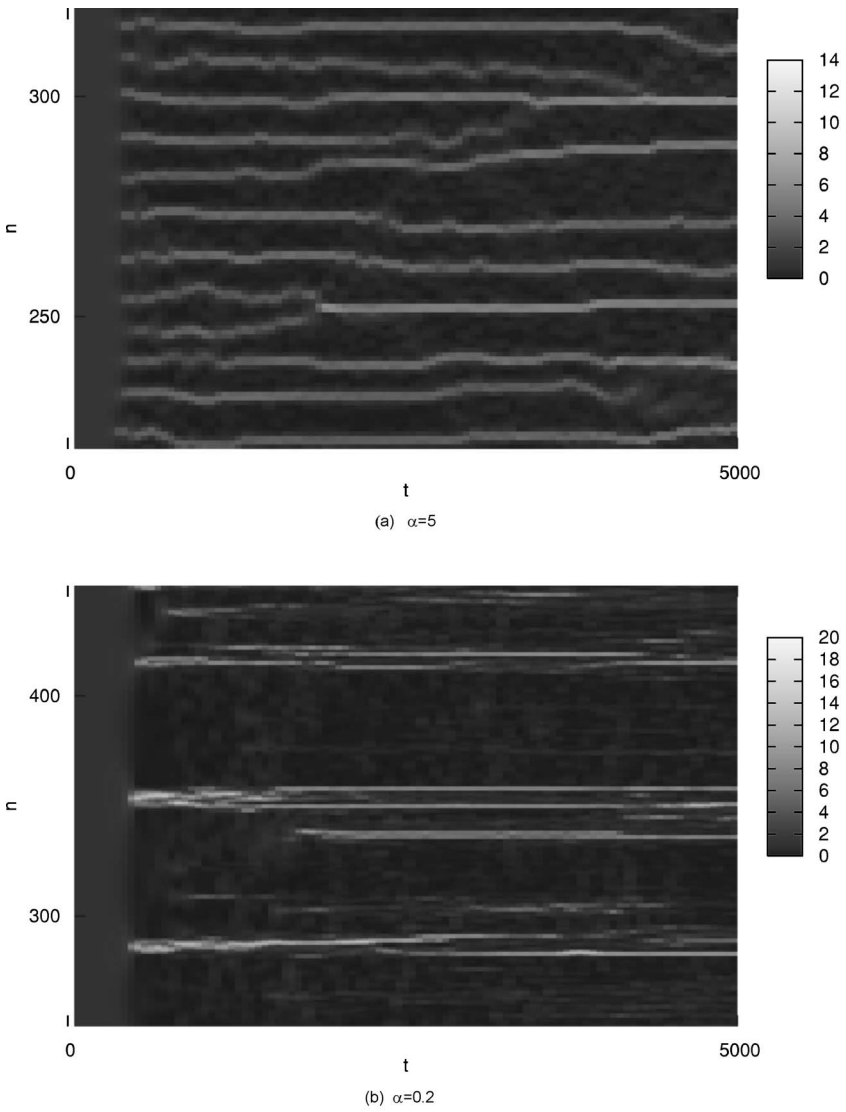

FIG. 4. Evolution of $|\phi_n|^2$ of the DNLS equation ($B=0.1$, $J=0.1$) without damping ($\gamma=0$) with $\alpha=5$ (a) and $\alpha=0.2$ (b) with the initial condition II and $a=0.16$. For the smaller value of α there are no collisions of breathers but longe-range transfer of energy/norm which leads to a somehow marbled pattern.

In the following, we measure $p(A)$ of the system (1) for $\alpha=5$, $\alpha=0.2$, and $\alpha=0.04$ in order to see the influence of the long-range forces on the thermalized system. In Fig. 5, we present the results for $p(A)$ for the undamped system of Fig. 4 after the system has reached thermal equilibrium which is indicated by constant mean values of $p(A)$ and η. We encounter some important changes for the different values of α:

The linear part of $p(A)$ (for small values of A) changes with decreasing α, which is not very surprising because β and μ will in general change with α. The linear region is clearly reduced to smaller values of A, which means that the Gibbsian part of the phase space ($\beta=0$), the regime of the low-amplitude excitations, has shrunk and the separation in low and high-amplitude regions is less pronounced for increasing long-range radius. For $\alpha=0.04$ the minimum of $p(A)$ for intermediate values of A has practically vanished. Moreover, the maximum peak height A of the breathers is distinctly enhanced and the course of $p(A)$ becomes quite irregular for large A. The main effect of the long-range interactions is obviously a flow of norm from the low-amplitude excitations to the intermediate and high-amplitude regime.

When we consider the effect of α on the thermalization of the system as in Fig. 5 by just changing the value of α, we have to admit that this procedure is qualitative because the Hamiltonian of the system depends also on α. However, in the case of initial conditions I or II the comparison in Fig. 5 is justified by the fact that under the constraint of a uniformly distributed norm, we put the α-independent maximum energy into the DNLS system. The initial conditions ($|\phi_n|=|A_n(t)e^{i\theta_n(t)}|=\sqrt{a}$) can only adopt energies H in an interval which depends on α. Proceeding as in [18] we can immediately specify the upper bound $-H^u$ (for $\phi_n(0)=\sqrt{a}$), the lower bound $-H^s(\alpha)$ [for $\phi_n(0)=\sqrt{a}\exp(i\pi)$], and the energy at the phase transition $-H_{\beta=0^+}$ (the minus signs appear because in [17,18] the opposite sign for the Hamiltonian (3) was used), see Fig. 6,

$$-h_{\beta=0^+}=-\frac{H_{\beta=0^+}}{N}=-Ja+\frac{3}{2}a^2, \tag{29}$$

$$-h^s(\alpha\to\infty)=-\frac{H^s(\alpha\to\infty)}{N}=-2Ja+\frac{3}{4}Ba^2, \tag{30}$$

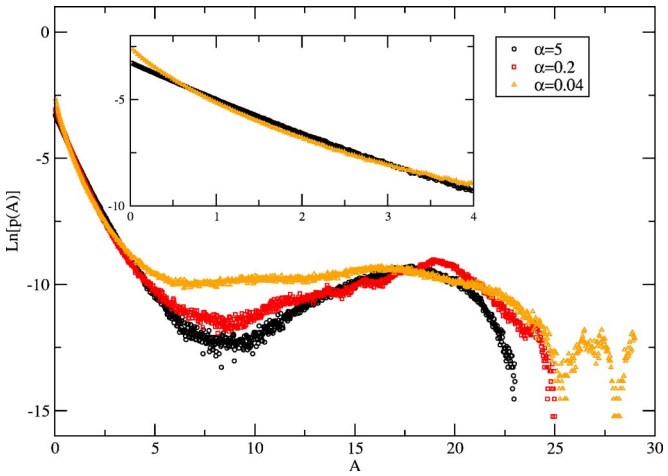

FIG. 5. (Color online) Time-averaged and normalized distribution function $p(A_n)$ for the DNLS with initial condition II with $a=0.16$. The data were obtained by averaging over 1000 time instants in a system of $N=4096$ lattice points ($\sim 4\times 10^6$ data points!) in a time period of $\sim 10^5$ after the quantity η reached a constant mean value. The simulations were performed for the values $\alpha=5$ (circles), $\alpha=0.2$ (squares), and $\alpha=0.04$ (triangles). The long-range scale α^{-1} has a strong influence on the profile of $p(A)$ even though the coupling $J(\alpha,N)$ becomes very small for small α.

$$-h^s(\alpha\to 0)=-\frac{H^s(\alpha\to 0)}{N}=-Ja+\frac{3}{4}Ba^2, \qquad (31)$$

$$-h^u=-\frac{H^u}{N}=\frac{3}{4}Ba^2. \qquad (32)$$

Only the lower bound of $-H$ depends on the long-range interaction. While the result for $-H^u$ can be immediately seen from (3), the result for $-H_{\beta=0^+}$ requires a calculation of the grand-canonical partition function of the DNLS in the limit $\beta\to 0^+$ (see Appendix).

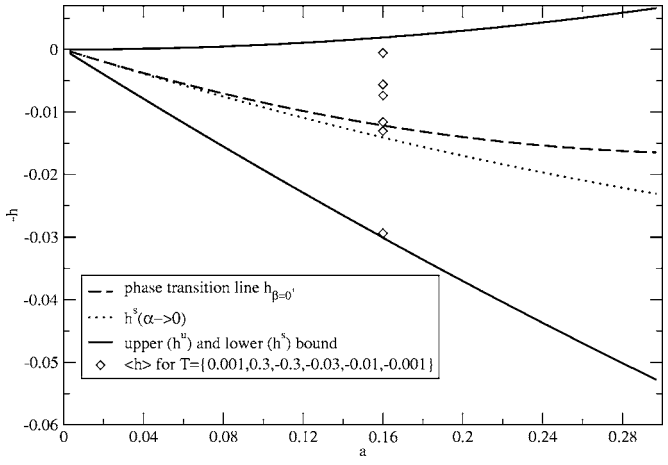

FIG. 6. The curves for the energy densities $-h=-H/N$ from (29)–(32) and the data points for the mean energy densities $\langle -h\rangle$ at the temperatures in Fig. 10 as a function of a for a system with $B=J=0.1$.

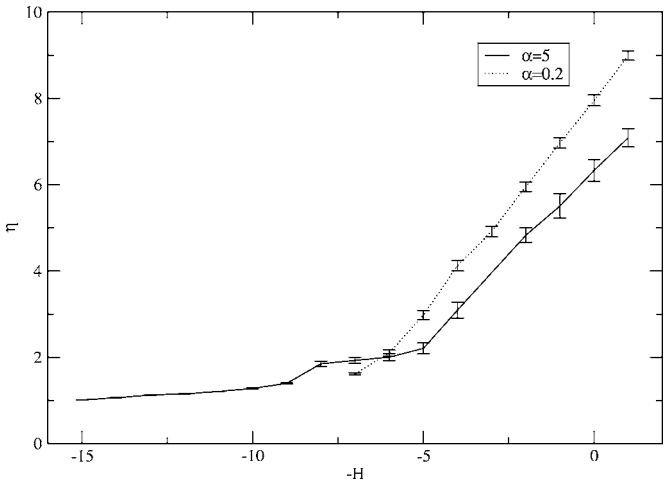

FIG. 7. Mean value of the norm localization η (1000 points) as a function of the system energy ($B=J=0.1$, $a=0.16$, $N=512$). The results in (33) for $\alpha\to 0$ or ∞ agree well with the values of H for $\alpha=5$ and 0.2. Only at the energy $H_{\beta=0^+}=-6.23$, the value of η is the same for every α.

In our simulations we restrict ourselves to the case $B=J=0.1$, $a=0.16$, and $N=512$. Then the energies take the values

$$-H_{\beta=0^+}=-6.23, \quad -H^s(\alpha\to\infty)=-7.21,$$

$$H^s(\alpha\to 0)=-15.40, \quad -H^u=0.98. \qquad (33)$$

In order to demonstrate this, we measure the value η for different energies of the system (Fig. 7). We manipulate only the phases θ_n of the lattice sites to conserve the uniform norm distribution for different energies. We can clearly see that for $\alpha=5$ and $\alpha=0.2$ the system energy lies in the predicted intervals (33) and the value of η at the phase transition energy does not depend on α, which confirms the calculation and interpretation of $H_{\beta=0^+}$ as the energy which corresponds to the limit of infinite temperature.

Concerning the thermodynamics of the DNLS, our goal in this context is to clarify the influence of the long-range forces on the localization strength η for a given temperature. Therefore we made a second series of η measurements, where the initial conditions were found by hybrid Monte Carlo simulations of the DNLS system. We manipulated again the phases θ_n in a random way (the norm is conserved) and accepted or rejected a new configuration with the probability $\exp(-\beta\Delta H)$. When the acception rate became very small, occasional deterministic simulations of the DNLS equation (1) were used to refresh the system. We used the Monte Carlo method for positive and *negative* temperatures. After many Monte Carlo steps, the system reaches states where the mean value of H is constant (Fig. 8). The Monte Carlo procedure confirmed the calculation of $-H_{\beta=0^+}$, meaning that for large positive or negative values of T ($\beta\to 0$) the energy of the system approached the value −6.23. We used these configurations as initial conditions for simulations of the DNLS system to measure $\eta(T)$. We found that the norm localization of the DNLS depends strongly on α in the negative temperature regime (Fig. 9).

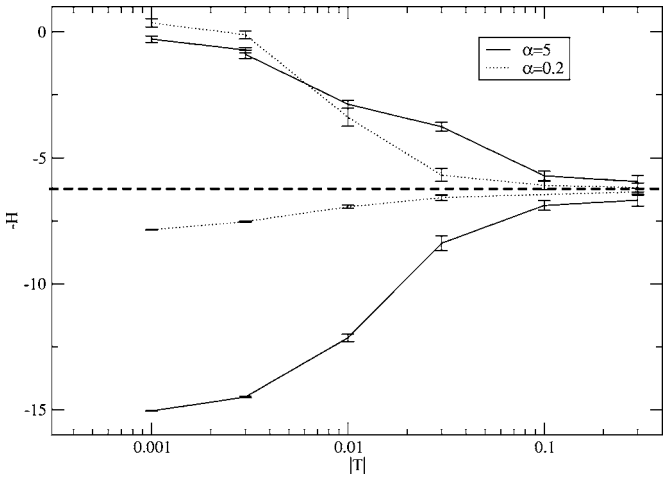

FIG. 8. The hybrid Monte Carlo simulations yield the mean values of the system energy (3), which are displayed for positive and negative temperatures, under and above the dashed line, respectively. For large positive and negative temperatures T (not shown), the algorithm leads independently of α to systems with $-H=-H_{\beta=0^+}=-6.23$ (the dashed line).

We want to mention that in the statistical mechanics approach we describe the system with only two parameters H and $\mathcal{N}$. The results (33) hold for arbitrarily extended initial conditions, e.g., the case of plane waves. In the literature [9], the modulational instability of plane waves was considered as a condition for energy localization in nonlinear lattices. For the DNLS system (1) (with $B,J>0$) modulational instability occurs for plane waves with $k\leqslant\pi/2$ for all values of α. The important point is that modulational instability does not lead to the formation of persistent breathers if the energy in the system does not suffice to cross the phase transition line $\beta=0^+$. So, a modulational instable planar wave is not a sufficient condition to obtain persistent breather formation. For example, we ran a simulation with an initial condition in form of a plane wave with $k=100/N\pi$ and the same $\mathcal{N}$ as for initial conditions II and I ($N=512$, $\mathcal{N}=Na$ with $a=0.16$). For $\alpha=5$ and $\alpha=0.2$ we have observed the modulational instability of the plane wave but the persistent breather formation occurs only for $\alpha=5$ because in this case we have an energy $-H$ larger than $-H_{\beta=0^+}$.

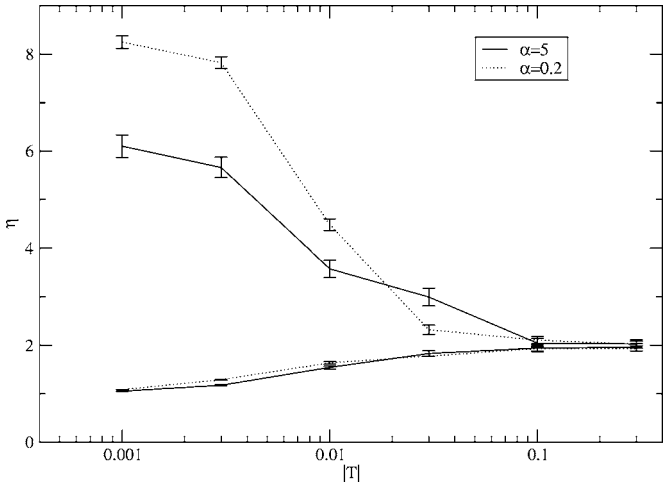

FIG. 9. Mean value of the norm localization η as a function of the system temperature ($B=0.1$, $J=0.1$, $N=512$). The initial conditions were created by Monte Carlo simulations of the DNLS system. The values above the high-temperature limit of the localization strength $\eta\approx 2$ correspond to negative temperatures and values below $\eta\approx 2$ correspond to positive temperatures for $\alpha=5$ and $\alpha=0.2$.

Contrary to what one might guess first, the parameter η behaves very smoothly at the transition line $\beta=0^+$ for $H=H_{\beta=0^+}$. The main influence of the long-range interaction is, apart from the fact that the positive temperature region is packed into a smaller energy interval, the distinctly higher values for the norm localization for $T\rightarrow -0$. In the simulation of the undamped system (1), we can directly monitor the formation of persistent breathers. When this is the case, we should observe that the probability of finding the norm of the system is larger for some sites than for others. This means, we should check if the values

$$p_n=\frac{|\phi_n|^2}{\mathcal{N}} \tag{34}$$

deviate from the value $1/N=1/512$ for negative temperatures. We can see in Fig. 10 that the values p_n behave rather smoothly at the phase transition line. For the values $T=0.3$ and $T=-0.3$, the site occupation probability p_n is extended in both cases and does not differ very much. The mechanism of the persistent breather formation starts at $H=H_{\beta=0^+}$ transferring energy into some hot spots. Therefore, we do not really expect drastic effects as long as we are close to the phase transition line, like for the temperatures $T=0.3$ and $T=-0.3$ (the two points in Fig. 6 next to the dashed line). For smaller negative values of T, we can clearly see the tendency to localize energy on certain sites. The occupation probability p_n at some lattice sites in Fig. 10 at $T=-0.001$, pretty close to the upper bound h^u, is already 20 times larger than for most of the other sites. The high-amplitude breathers are pinned because a hopping to a neighboring site is not possible since the bond cannot store such large amounts of energy [21]. The long-range forces (small α) lead to the tendency to store more norm in high-amplitude excitations, which means for the site-occupation probability p_n that there are more (and higher) peaks on a slightly lower small-amplitude background.

VII. CONCLUSIONS

In the first part of the paper we could show that long-range forces combined with norm-conserving damping leads to the formation of a very regular array of stationary breather solutions starting from a spatially extended state. The tendency of energy localization depends strongly on the long-range terms and the damping acts as a promoter. We were able to explain the dependence of the mean breather distance on the long-range parameter and gave a qualitative explanation of the norm localization mechanism in the early state of the system using the dimer approximation. We want to mention that the nonlinear damping was not chosen arbitrarily

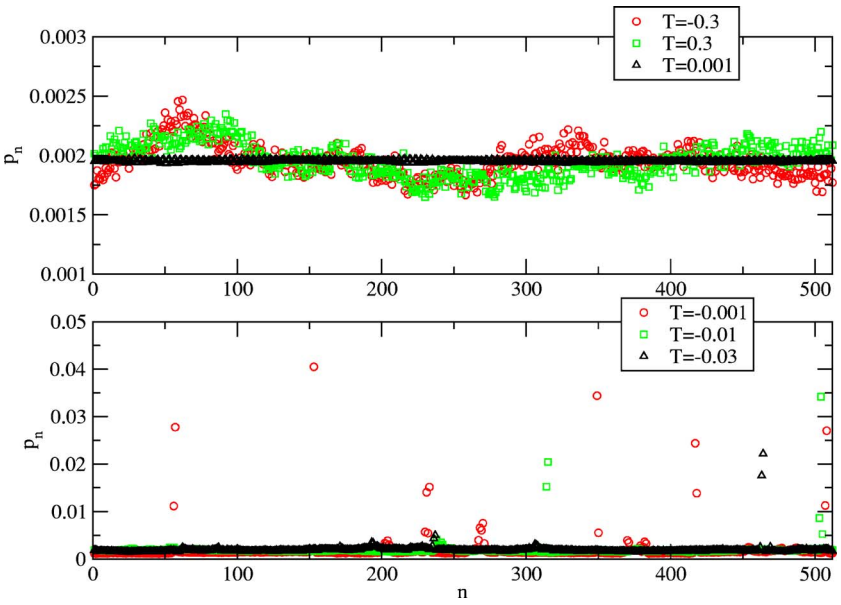

FIG. 10. (Color online) The mean values of the site occupation probability p_n ($B=0.1$, $J=0.1$, $N=512$, $\alpha=5$) for six different temperatures [upper panel: $T=-0.3$ (circles), $T=0.3$ (squares), $T=0.001$ (triangles); lower panel $T=-0.001$ (circles), $T=-0.01$ (squares), $T=-0.03$ (triangles)].

but stems from a dissipative term in the Davydov equations. In the case of small damping ($\gamma < B, J$), the transition to the stationary state takes longer. The influence of long-range interactions was found to be crucial, even for very small coupling strength, provided that the radius of the interaction is large in comparison with the lattice spacing, which should be true for many models e.g. those of biomolecules. Effects of additional noise on a single DNLS breather in the DNLS with nonlinear damping were investigated in [12], but the role of noise for the formation of the persistent breathers is still an open question.

In the second part, when we do not assume any damping mechanism and the energy of the DNLS is a second conserved quantity, high and low-amplitude excitations are in thermal equilibrium. We showed that the high-temperature limit is independent of the long-range interactions and only the lower bound of the energy is changed. The simulations prove that the long-range forces lead to an effective norm transfer from low- to high-amplitude excitations, which yields a higher norm localization. Using Monte Carlo techniques (which agree with the analytical result for $H_{\beta=0^+}$), we were able to identify the dependence of the energy and the norm localization on the temperature of the system. The transition to the persistent breather regime was found to be rather smooth for small α, but for the limit $T \to 0^-$, the long-range character of the system enables a distinctly higher degree of localization.

A Java-Applet for a small DNLS-system consisting of 64 sites is accessible at http://www.phy.uni-bayreuth.de/~btp342/DNLS.html

APPENDIX: GRAND-CANONICAL PARTITION FUNCTION

The Hamiltonian (3) in action-angle variables $A_n(t)$ and $\theta_n(t)$ takes the form

$$H = J\mathcal{N} - \sum_{n=1}^{N}\sum_{m=1}^{N} J\frac{(e^{\alpha}-1)}{(1-e^{-\alpha N})}e^{-\alpha m}\sqrt{A_n A_{n+m}} \times \cos(\theta_n - \theta_{n+m}) - \sum_{n=1}^{N}\frac{3}{4}BA_n^2. \tag{A1}$$

The Hamiltonian $-H$ is bounded from below by the staggered plane wave $\phi_n^s = \sqrt{a}e^{in\pi}$ which yields an α dependent minimum for $-H$,

$$H^s(\alpha) = 2J\mathcal{N}\frac{e^{\alpha}}{e^{\alpha}+1} - \frac{3}{4}BNa^2. \tag{A2}$$

For $\alpha=0.2$ the value of the lower bound of $-H$ lies at ≈ -7 while it is ≈ -15 for $\alpha=5$.

The grand-canonical partition function of the DNLS is defined as

$$\begin{aligned} Z &= \int_0^{\infty}\int_0^{2\pi} d\theta^N dA^N e^{\beta(H-\mu\mathcal{N})} \\ &\overset{(A1)}{=} \int_0^{\infty}\int_0^{2\pi} d\theta^N dA^N e^{\beta J\mathcal{N}} \prod_n^N e^{\beta(-3/4BA_n^2-\mu A_n)} \\ &\quad \times \prod_m^N e^{-J_m e^{-\alpha m}\sqrt{A_n A_{n+m}}\cos(\theta_n-\theta_{n+m})} \\ &= e^{\beta J\mathcal{N}} \int_0^{\infty}\int_0^{2\pi} dA^N \prod_n^N e^{\beta(-3/4BA_n^2-\mu A_n)} \\ &\quad \times \prod_m^N 2\pi I_o(-\beta J_m e^{-\alpha m}\sqrt{A_n A_{n+m}}), \end{aligned} \tag{A3}$$

where $I_o(z) = \frac{1}{\pi}\int_0^{\pi} e^{z\cos\theta} d\theta$ is the modified Bessel function of the first kind. The procedure of calculating the phase transition line in [18] is also valid for a system with long-range

forces when we consider the limit $\beta=0^+$, $\mu=\infty$ with $\beta\mu=\Gamma$ finite. In this limit we can assume $I_o\approx 1$,

$$Z^{\beta^{0^+}} \approx e^{\beta J\mathcal{N}}\left((2\pi)^N\int_0^\infty dx e^{-\mu\beta x}\left(1-\frac{3}{4}\beta B x^2\right)\right)^N$$
$$\approx (2\pi)^{2N}e^{\beta J\mathcal{N}}\frac{1}{(\mu\beta)^N}\left(1-\frac{3}{4}\beta B\frac{2}{(\beta\mu)^2}\right)^N. \quad \text{(A4)}$$

The average energy and norm in the canonical ensemble read

$$-H_{\beta=0^+}=\left(\frac{\mu}{\beta}\frac{\partial}{\partial\mu}-\frac{\partial}{\partial\beta}\right)\ln Z=-J\mathcal{N}+\frac{3}{2}NB\frac{1}{(\beta\mu)^2} \quad \text{(A5)}$$

$$\mathcal{N}=-\frac{1}{\beta}\frac{\partial\ln Z}{\partial\mu}=\frac{N}{\beta\mu}-\frac{3NB\beta}{(\mu\beta)^3}. \quad \text{(A6)}$$

We neglect the second term in $\langle\mathcal{N}\rangle$ and find the $\beta=0^+$-transition line in the (h,a) phase space

$$-h_{\beta=0^+}=-Ja+\frac{3}{2}Ba^2, \quad \text{(A7)}$$

where $-h=-H/N$ and $a=\mathcal{N}/N$ are mean energy and norm per site (see Fig. 6). In our simulations ($a=0.16$, $J=B=0.1$, $N=512$) we expect the phase transition at an energy of

$$-H_{\beta=0^+}=-6.23, \quad \text{(A8)}$$

which is marked by the dashed line in Fig. 8.

[1] A. Scott, *Nonlinear Science* (Oxford University Press, Oxford, 1999).
[2] G. Kopidakis and S. Aubry, Phys. Rev. Lett. **84**, 3236 (2000).
[3] A. Smerzi and A. Trombettoni, Chaos **13**, 766 (2003).
[4] A. Campa and A. Giansanti, Phys. Rev. E **58**, 3585 (1998).
[5] S. F. Mingaleev, P. L. Christiansen, Yu. B. Gaididei, M. Johansson, and K. Ø. Rasmussen, J. Biol. Phys. **25**, 41 (1999).
[6] A. C. Scott, Phys. Rep. **217**, 1 (1992).
[7] A. A. Sukhorukov, Y. S. Kivshar, H. S. Eisenberg, and Y. Siberberg, IEEE J. Quantum Electron. **39**, 31 (2003).
[8] A. J. Leggett, Rev. Mod. Phys. **73**, 307 (2001).
[9] J. C. Eilbeck and M. Johansson, in Proceedings of the Third Conference on Localization and Energy Transfer in Nonlinear Systems, June 17–21, San Lorenzo de El Escorial, Madrid, edited by L. Vázquez, R. S. MacKay, and M. P. Zorzano (World Scientific, Singapore, 2003), pp. 44–67.
[10] P. G. Kevrekidis, K. Ø. Rasmussen, and A. R. Bishop, Int. J. Mod. Phys. B **15**, 2833 (2001).
[11] O. Bang, P. L. Christiansen, F. If, K. Ø. Rasmussen, and Y. B. Gaididei, Phys. Rev. E **49**, 4627 (1994).
[12] P. L. Christiansen, Yu. B. Gaididei, M. Johansson, and K. Ø. Rasmussen, Phys. Rev. B **55**, 5759 (1997).
[13] Y. B. Gaididei, S. F. Mingaleev, and P. L. Christiansen, Phys. Rev. E **62**, R53 (2000).
[14] Y. B. Gaididei, N. Flytzanis, A. Neuper, and F. G. Mertens, Physica D **107**, 83 (1997).
[15] P. L. Christiansen, Y. B. Gaididei, F. G. Mertens, and S. F. Mingaleev, Eur. Phys. J. B **19**, 545 (2001).
[16] K. Ø. Rasmussen, S. Aubry, A. R. Bishop, and G. P. Tsironis, Eur. Phys. J. B **15**, 169 (2000).
[17] K. Ø. Rasmussen, T. Cretegny, P. G. Kevrekidis, and N. Grønbech-Jensen, Phys. Rev. Lett. **84**, 3740 (2000).
[18] M. Johansson and K. Ø. Rasmussen, Phys. Rev. E **70**, 066610 (2004).
[19] B. Rumpf and A. C. Newell, Phys. Rev. Lett. **87**, 054102 (2001).
[20] B. Rumpf, Phys. Rev. E **69**, 016618 (2004).
[21] B. Rumpf, Phys. Rev. E **70**, 016609 (2004).
[22] J. C. Eilbeck, P. S. Lomdahl, and A. C. Scott, Physica D **16**, 316 (1985).
[23] H. Feddersen, Phys. Lett. A **154**, 391 (1991).
[24] J. Edler, P. Hamm, and A. C. Scott, Phys. Rev. Lett. **88**, 067403 (2002).
[25] *Dynamics and Thermodynamics of Systems with Long-Range Interactions*, Lecture Notes in Physics 602, edited by Dauxois, Ruffo, Arimondo, Wilkens (Springer, New York, 2002).
[26] Y. S. Kivshar and M. Peyrard, Phys. Rev. A **46**, 3198 (1992).
[27] P. L. Christiansen, Yu. B. Gaididei, M. Johansson, K. Ø. Rasmussen, and I. I. Yakimenko, Phys. Rev. E **54**, 924 (1996).
[28] Yu. B. Gaididei, S. F. Mingaleev, P. L. Christiansen, K. Ø. Rasmussen, Phys. Lett. A **222**, 152 (1996).
[29] M. Johansson and S. Aubry, Phys. Rev. E **61**, 5864 (2000).
[30] T. Dauxois and M. Peyrard, Phys. Rev. Lett. **70**, 3935 (1993); O. Bang and M. Peyrard, Phys. Rev. E **53**, 4143 (1996); M. Peyrard, Physica D **119**, 184 (1998).
[31] T. Cretegny, T. Dauxois, S. Ruffo, and A. Torcini, Physica D **121**, 109 (1998).